Preparation, Properties, and Anticorrosion Application of Poly(methyl methacrylate)/Montmorillonite Nanocomposites Coating on Brass via Solution Polymerization

Tien-Li Wang, Weng-Sing Hwang, Meng-Heng Yeh

Department of Materials Science and Engineering, National Cheng Kung University, Tainan 701, Taiwan

Received 13 June 2006; accepted 21 November 2006
DOI 10.1002/app.26027
Published online in Wiley InterScience (www.interscience.wiley.com).

ABSTRACT: The aim of this study is to improve the anticorrosive property of 7Cu3Zn brass. The methyl-methacrylate (MMA) monomer solution, modified with fluorine radical and silicone, was used as the polymer matrix to mix with the different percentages of modified montmorillonite (MMT) loading and to exfoliate the lamellar structure of MMT on a nanometer scale during the solution polymerization process, and then form a thin nanocomposites coating on brass as a protective layer. The structural characterization was examined using Fourier transform infrared spectroscopy, X-ray diffraction (XRD), and transmission electron microscope (TEM). The anticorrosive property of nanocomposites was evaluated using potentiodynamics polarization and electrochemical impedance spectra. The results show that the *d*-spacing of MMT was increased, and both exfoliation and intercalation microstructure were observed. Moreover, with the MMT loading increase, the appearance of the intercalation microstructure was more remarkable as a result of silicate layers aggregation. The 1.0 wt %-coated brass coupons presented the optimistic property of anticorrosion, whose oxygen permeability, corrosion current (i_{corr}), polarization resistance (R_p), and corrosion rate (R_{corr}) were 3.5 g/(m^2°h), 6.86 nA/cm^2, 5.81×10^5 Ω°cm^2, and 0.103×10^{-3} mm/year, respectively. These results indicate that nanocomposites have potential for anticorrosion application. © 2007 Wiley Periodicals, Inc. J Appl Polym Sci 104: 4135–4143, 2007

Key words: PMMA/MMT; exfoliation; gas barrier; corrosion current; TEM

INTRODUCTION

Brass, an alloy of copper and zinc, has been widely used as tubing material for condensers and heat exchangers in various water cooling systems. With the zinc content of brass below 39%, zinc dissolves in copper and forms α solid solution, which exhibits excellent ductility and working ability. Hence, this kind of brass, such as 7Cu3Zn, is often used to manufacture the complicated-shaped molding product. However, brass is susceptible to a corrosion process known as dezincification and this tendency increases in proportion to the greater amount of zinc content. During the past decade, many techniques have been used to minimize the dezincification and corrosion rates of brass.

An organic inhibitor is often used to minimize the corrosion susceptibility of brass by the formation of an insoluble and polymeric film,[1] whereas polymer coating, as a physical barrier, is also able to efficiently minimize the corrosion rate of the metal.[2]

Moreover, according to the studies on nylon-6/montmorillonite (MMT) nanocomposite by Toyota Motor,[3–5] silicate layers of MMT could be well-dispersed in a polymer matrix on a nanometer scale. Following upon this development, polymer/MMT nanocomposites have been reported to boost the thermal stability, mechanical properties, flame resistance, gas barrier, and corrosion inhibition. Particularly, anticorrosion application based on coupling a polymer with MMT has been studied on poly-(methyl methacrylate) (PMMA),[6] polyimide,[7] polyaniline.[8] Generally, these materials were produced by melt intercalation of thermoplastic, bulk polymerization, or *in situ* polymerization.[6] In this study, solution polymerization is employed since its lower molecular weight (M_w), lower viscosity, better filling and floating ability for complicated-shaped metal surface, all suit the requirements of coating materials.

MMT, with dimensions of $100 \times 100 \times 1$ nm^3, has high in-plane strength, stiffness, and a high aspect ratio. Typically, MMT is composed of two fused tetrahedral silica sheets sandwiching an edge-shared octahedral sheet. Isomorphous substitutions of Si^{4+} for Al^{3+} in the tetrahedral lattice and of Al^{3+} for Mg^{2+} in the octahedral sheet cause an excess of negative charges within the MMT layers. These negative

Correspondence to: W.-S. Hwang (wshwang@mail.ncku.edu.tw).

Journal of Applied Polymer Science, Vol. 104, 4135–4143 (2007)

charges are counterbalanced by cations such as Ca^{2+} and Na^{+} situated between the MMT layers, which are hydrophilic in polar solution. Because of this, organic surfactant of the layered MMT is required for modifying MMT's compatibility with most polymers. As a result, the organophilic MMT is able to couple with a polymer and further exfoliate its lamellar structure during the polymerization process, ending in nanocomposites. Generally, phase separation, intercalation, and exfoliation are three types of microstructures of polymer/MMT nanocomposites. It is believed that exfoliation of the MMT layers leads to the best anticorrosive property and the lowest gas permeability.[6,7,9]

PMMA is a transparent, hard, and stiff material with excellent ultraviolet stability, low water absorption, and outstanding outdoor weathering properties. The studies on PMMA/MMT nanocomposites have mainly been directed toward the elucidation of the effect of the inclusion of MMT on thermal properties,[10] barrier properties,[11] the characterization of the nanometer structures, and anticorrosion of cold-roll-steel.[6,7,9] However, there have been few studies on the effect of MMT loading on the microstructure of nanocomposites or on minimizing the corrosion rate of brass.

Therefore, the aim of this study is to improve the anticorrosive property of 7Cu3Zn brass by coating if with PMMA/MMT nanocomposites. Following this, the characterization, morphology, *d*-spacing, inner microstructure, and anticorrosive property of nanocomposites are examined and elucidated in the following sections. Moreover, the potential of polymer/MMT nanocomposites coating should not be underestimated because they provides us with a much cleaner way to minimize corrosion than do chromate compounds, which although are excellent anticorrosive inhibitors, have been restricted worldwide as they are considered highly toxic and carcinogenic.

EXPERIMENTAL

Experimental process

The experimental method used a methyl-methacrylate (MMA) monomer solution, modified with fluorine radical and silicone, as the polymer matrix to mix with different percentages of modified MMT loading and to further exfoliate the silicate layers of MMT during the solution polymerization process on a nanometer scale. Finally, the thin PMMA/MMT nanocomposites coating is formed on a brass surface. Then, the characterization, *d*-spacing, and inner microstructure of nanocomposites were examined using Fourier transform infrared (FTIR) spectroscopy, X-ray diffraction (XRD), and transmission electron microscope (TEM), respectively. The anticorrosive property of nanocomposites was evaluated using potentiodynamics polarization and electrochemical impedance spectra (EIS).

Modification of MMT

In this study, the Na^{+} existing in the interlayer regions are replaced by lauryl amine through a cationic-exchange reaction to render the hydrophilic layer silicate organophilic.

The quantity of the intercalating agent used for the cation-exchange reaction is given by:

$$X = 114/100 \times 30 \times 1.3 \times M_w/1000 \qquad (1)$$

where X is the weight in grams of the intercalating agent when 30 g of MMT clay is used, 114/100 is the cation exchange capacity per 100 g of MMT, 1.3 is the excess amount of intercalating agent used, M_w is the molecular weight of the intercalating agent, and 1000 is used to balance the units.[12]

The present experimental setup was comprised of three main components: (1) a stirring system composed of a stirring machine, a thermometer, a nitrogen gas supply, and a three-necked round-bottomed flask, (2) a heating system, containing a heater, a pan and silicon oil, and (3) a filter, comprising of a funnel, a vacuum flask and a mechanical pump.

To modify the MMT, solutions comprising of MMT, modifier, and HCl were dispersed in highly resistive water in the three-necked flask. Nitrogen gas was bubbled into the flask throughout the reaction processes. While being stirred continuously at 500 rpm, the solutions were maintained at a temperature of 80°C for 3 h. The resulting suspensions were then filtered, and the solid residues rinsed with water to remove all traces of chloride, as determined by a silver nitrate test. The products were then dried at 80°C for 24 h in a convection oven, milled with a ball end mill, and finally sintered with a 325-mesh net to yield the final modified clay sample.

Preparation of PMMA/MMT nanocomposites by solution polymerization

Solution polymerization is used with its advanced filling and floating abilities because propagation of polymerization is initiated by a monomer solution, leading to a smaller molecular weight (M_w) and lower viscosity. Hence, with these characteristics, better forming ability and thinner thickness can be achieved by solution polymerization, thus suiting the vital requirements of coating materials.

PMMA/MMT nanocomposites were prepared by the solution dispersion method. MMA monomers/PMMA solution consisted of 44.3% butyl acetate solvent, 42% MMA/PMMA (4261A-(5H-6H), from Eternal), 13.6% Bayer *N*-3390 curing agent, and 0.1%

dibutyltin dilaurate (DBTL) catalyst. The composition ratios of the solution/MMT were: 100/0, 99.5/0.5, 99.25/0.75, 99/1.0, 98/2.0, 97/3.0, and 95/5.0 w/w.

A typical procedure for preparing nanocomposites incorporated with 1 wt % MMT is described as follows: Firstly, 0.10 g of organophilic MMT was suspended into 7.95 g of MMA/PMMA solution without curing agent, Bayer *N*-3390, in the reaction flask under magnetic stirring at room temperature for 15 h, forming a well-dispersed lacteous solution. After this, 1.95 g of *N*-3390 was introduced into the flask under magnetic stirring for 30 min at room temperature. During mixing, the crosslinking process and polymerization of MMA/PMMA immediately took place. Then, the optimum crosslinking amount of PMMA/MMT nanocomposites solution could be obtained; this solution should be immediately used in mechanical or anticorrosive applications in case it would eventually be completely crosslinked and solidified.

Preparation of nanocomposites coating on brass

Nanocomposites coating on brass were prepared via dipping method. The exposed surface area of the brass coupon for coating is 1.5 cm × 1.5 cm. Each brass coupon was abraded mechanically with silicon carbide papers from 120 to 1000 grit, and then was thoroughly washed with distilled water, degreased in acetone for 15 min using ultrasonic vibration, rinsed with distilled water, and dried. Following this, one side of the brass coupon was blanketed with adhesive tape, then dipped into PMMA/MMT nanocomposites solution, although not completely crosslinked yet, for 30 s, and cured in the oven for 6 h at 50°C to evaporate the superfluous organic solvent and to complete polymerization. Subsequently, PMMA/MMT nanocomposites coating on the other side of the brass coupon was formed. The brass coupon was mounted onto the working electrode so that only the coated side was in direct contact with the electrolyte. As in the typical procedure of preparing a working electrode, the uncoated side of the brass coupon and the electric cord were combined together and then sealed with super fast epoxy cement for insulation with electrolyte.

Examination of nanocomposites

To investigate the bonding between the MMT and the surfactants, the powdered organophilic MMT compound was mixed with KBr powder, then reground and pressed into a single pellet. Its bonding was then examined with a BIO-RAD FTS-7 FTIR spectrometer.

An XRD study of the samples was carried out using a diffractometer (D-max/IIV, Rigaku, Japan) with a copper target and Ni filter to measure the interclay *d*-spacing of the MMT samples at a scanning rate of 1°/min by monitoring the diffraction angle(2θ) from 2 to 10°.

The microstructure and dispersion of nanocomposites were examined using transmission electron microscopy (TEM) to determine the internal micrograph. First, the process of TEM samples was prepared by half filling low viscosity embedding media capsules and by curing the half-filled media at 60°C for 72 h in an oven. Then a thin film of PMMA/MMT nanocomposites was put on the half media and cured in the oven for 6 h at 50°C, followed by another half of the same embedding media being filled and then cured at 60°C for 72 h in an oven. Following this, the cured capusules containing the PMMA/MMT nanocomposites were microtomed cryogenically with a Leica Ultracut Uct into 50-nm-thick slices. Subsequently, these slices were collected on 100-mesh copper nets for TEM observation on a JEM-2010 Electron Microscope (JEOL Co. 200 KV)

Gas permeability of nanocomposites was examined using the Yanco GTR-10 gas permeability analyzer. As with the process of PMMA/MMT nanocomposites solution above, this solution was then cast uniformly on substrate (e.g., a microscope glass slide). The solvent was allowed to evaporate at 50°C in the oven for 6 h. Then, the sample-coated glass substrate was immersed in distilled water for 6 h to provide the membrane of PMMA/MMT with the nanocomposites.

The rate of transmission of oxygen was obtained using gas chromatography, and from the results, the air permeability was calculated. Meanwhile, a water vapor permeability examination was performed by the same experimental method.

To investigate the anticorrosive property of brass coated with nanocomposites, a salt bath and electrochemical corrosion measurements were employed. The salt bath was examined using ERICHSEN rKc CB500 to observe and record the progress of brass surface corrosion at a temperature of 40°C. The electrochemical corrosion measurement consisted of potentiodynamic polarization and EIS. A conventional three-electrode electrochemical cell, which consisted of the brass coupon with an exposed surface area of 1.5 cm × 1.5 cm as the working electrode, a platinum mesh (6 × 6 cm^2) as counter electrode, and a saturated calomel electrode (SCE) as reference electrode with a Luggin capillary probe, was filled with 500 mL NaCl (5 wt %) aqueous electrolyte. Potentiodynamic polarization studies were carried out using potentiostat/galvanostat (Model 263A EG and G instruments). The experimental set is shown in Figure 1. The working electrode was immersed in electrolyte and allowed to stabilize for 30 min. The open-circuit potential at the equilibrium state of the system was recorded as the ideal corrosion potential (E_{corr} in volts versus SCE). The cathodic and anodic

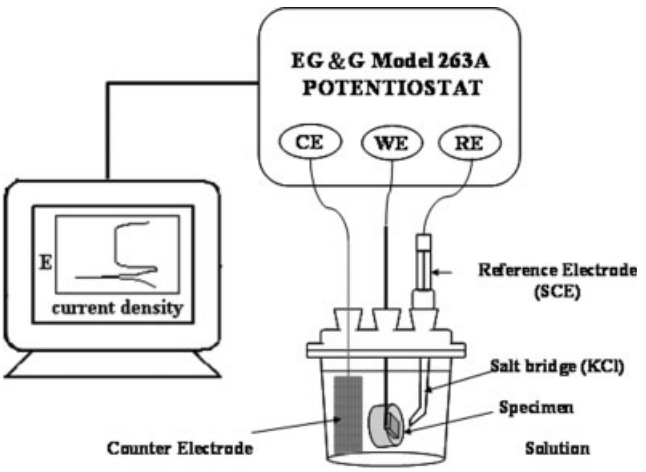

Figure 1 Experimental set of electrochemistry measurement.

polarization curves (Tafel plot) of the brass coupon were measured by sweeping the applied potential from −600 to 200 mV versus SCE at a scan rate of 0.5 mV/s. With the incorporation of an A. C. impedance analyzer (Schlumberger SI 1255) and a Schlumberger Solartron 1250 HF FREQUENCY RESPONSE ANALYZER, EIS studies were acquired in the frequency range from 65,535 to 0.001 Hz, with a 10 mV amplitude sine wave generated by a frequency response analyzer.

The anticorrosive property of the brass coupon was mainly evaluated by corrosion current density (i_{corr}) using the Tafel extrapolation method and polarization resistance (R_p). According to the corrosion current, the corrosion rate (R_{corr}, mm/year) was calculated from[2]

$$R_{corr} = \frac{3.27 \times 10^3 \times I_{corr} \times EW}{D} \quad (2)$$

where EW is the equivalent weight (in g/eq.), and D is the density (in g/cm^3). All the experiments were performed under controlled conditions. All data was replicated at least three times to ensure reproducibility and statistical significance.

RESULTS AND DISCUSSION

Structural characterization of modified MMT

FTIR was employed to analyze the bonding between MMT and the surfactant. Figure 2 shows the infrared spectrograph of unmodified MMT and modified MMT. The MMT bonded at 1040 cm^{-1} (Si—O), 600 cm^{-1} (Al—O), and 420 cm^{-1} (Mg—O). The surfactant Lauryl amine ($C_{12}H_{27}N$, M_w 185) bonded at 850 and 2920 cm^{-1} for CH_2. From these results, it can be seen that the surfactant bonded with MMT and modified the hydrophilic MMT so that it became compatible with the organic solution as organophilic MMT.

The XRD patterns of MMT, modified MMT, and nanocomposites are shown in curves (g) and (h) of Figure 3. The (001) d-spacing of the SiO_2 sheets in MMT was 1.28 nm. After modification by lauryl amine, the d-spacing increased to 1.7 nm and the peak was also shaped.[13]

Dispersion of modified MMT in PMMA

According to Figure 3, there is no peak in curves (a–e), indicating the fact that the silicate layers of modified MMT were possibly exfoliated in the PMMA matrix. However, in curve (f), two peaks at 2θ = 3.04 and 6.31° can be found, which implies the possibility that modified MMT could not be exfoliated completely in the PMMA matrix and consequently existed in intercalation, or even phase separation.

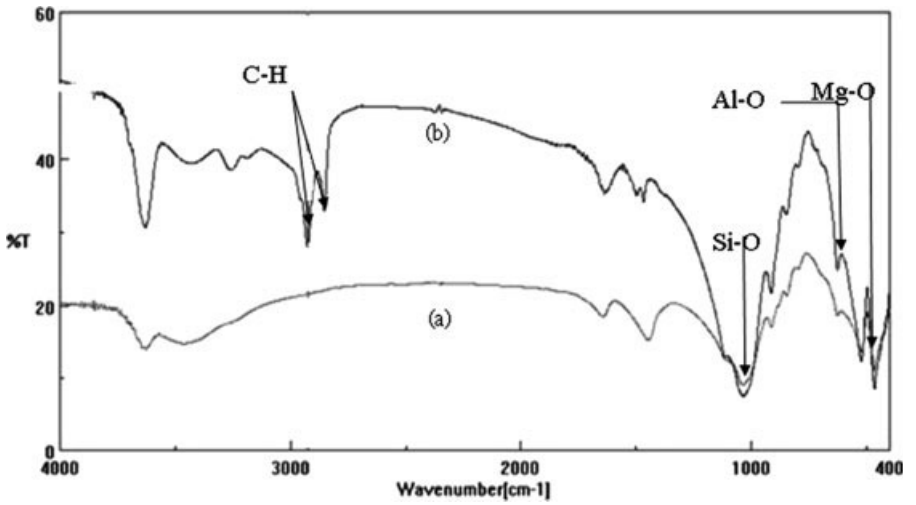

Figure 2 FTIR of (a) unmodified MMT, (b) organophilic MMT.

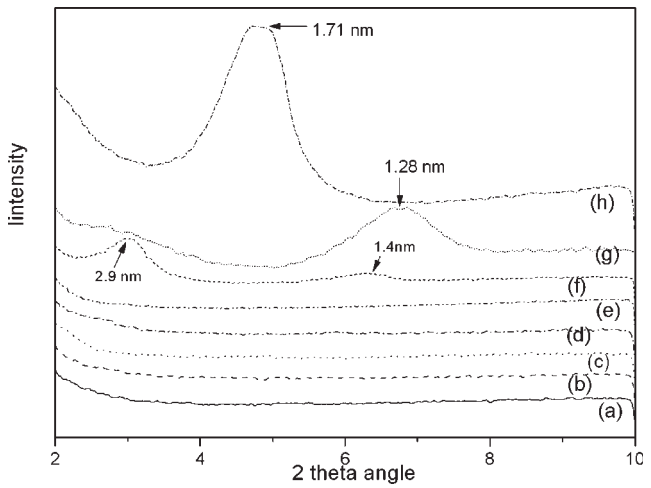

Figure 3 XRD diffraction patterns containing (a) 0.5 wt %, (b) 0.75 wt %, (c) 1.0 wt %, (d) 2.0 wt %, (e) 3.0 wt %, (f) 5.0 wt % of modified MMT, (g) modified MMT, and (h) MMT. XRD diffraction was performed using an X-ray wavelength of 1.541 Å.

Since the microstructure and dispersion of PMMA/MMT nanocomposites should be known, TEM micrograph was employed. In Figure 4(a,b), TEM micrographs of nanocomposites of capsules with 2.0 wt % modified MMT loading show that the nanocomposites exhibited a mixed nanomicrostructure of exfoliation and intercalation. Because the silicate layers were composed of heavier elements (Al, Si, and O) than the interlayer and surrounding matrix (C, H, and N), MMT silicate layers appeared darker in the bright-field images. In Figure 4, individual silicate layers, along two, three and more layer stacks, were found to be well-dispersed in the PMMA matrix. Moreover, some larger intercalated or aggregated tactoids could also be identified. In Figure 4(a), most of MMT silicate layers were exfoliated separately, and the distance between them were larger than 20 nm. The aggregation area was also found. The block-shaped darker area is shown in Figure 4(a). In Figure 4(b), the exfoliation area still could be found, and moreover, the intercalation area was also identified. Three to seven layers of silicate were intercalated together and the distance between each layer is about 3 nm. As a result, exfoliation and intercalation could be found in nanocomposites with 2.0 wt % modified MMT loading, indicating that the lamellar structure of MMT could not be exfoliated completely during the polymerization process.

Moreover, on the basis of the multipoint observation by TEM, the intercalation or even aggregation, was observed more frequently in the sample of 2.0 wt % than the one of 0.75 wt%. It means that as the amount of modified MMT increased, MMT had a tendency to aggregate together.[14–16] This shows that the MMA monomer did not diffuse into all of the modified MMT galleries,[14] and that the *d*-spacing and organic compatibility of modified MMT were unable to react completely during the polymerization process. Consequently, some of these silicate layers would aggregate together by PMMA molecules swelling during the polymerization progress. The intercalation and aggregation locations would

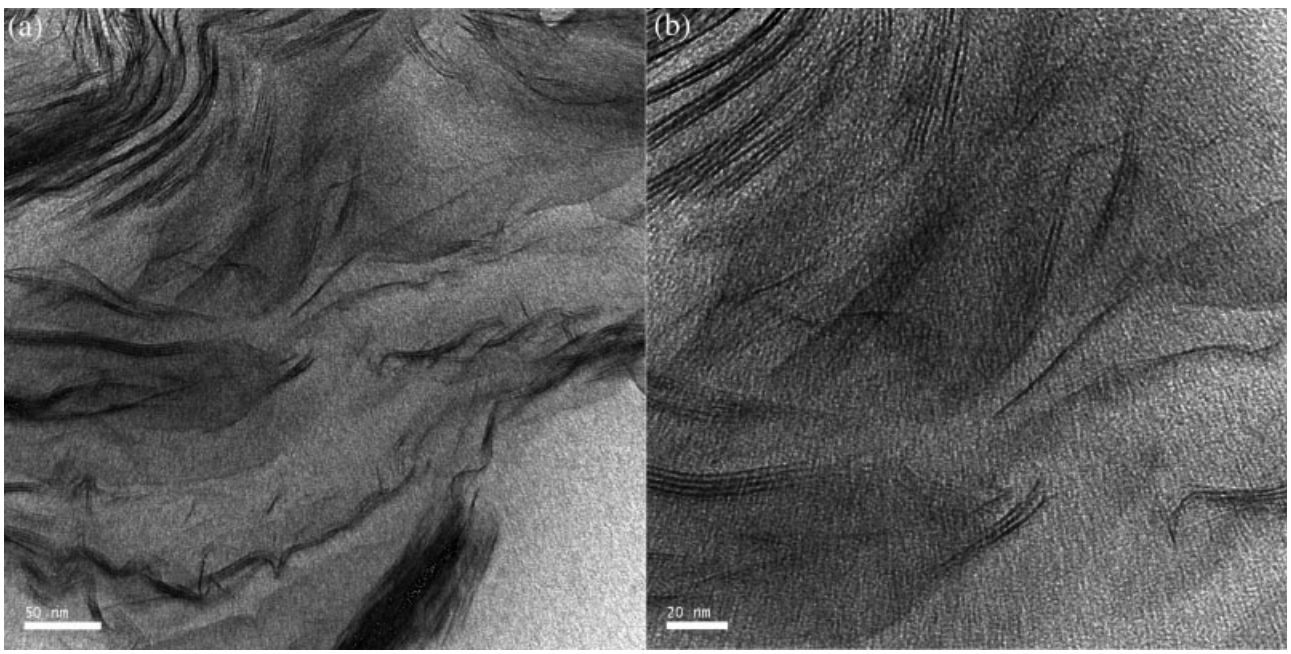

Figure 4 (a) TEM of MMT loading at 2.0 wt %, with aggregation, intercalation, and exfoliation. Most of the MMT has departed into intercalation and exfoliation. (b) TEM of MMT loading at 2.0 wt %, with intercalation and exfoliation. It was observed that there are separated-silicate layers, and 3–8 layers were intercalated together.

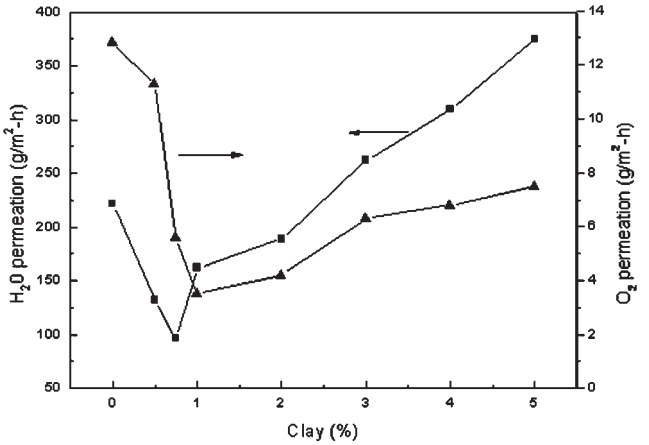

Figure 5 Permeability of H_2O vapor and oxygen as a function of MMT loading in the PMMA/MMT nanocomposites.

induce stress concentration,[14] which may increase the corrosion susceptibility and decrease the anticorrosive property of brass coated with PMMA/MMT nanocomposites. Hence, the influences on the anticorrosive property of nanocomposites resulting from unexpected intercalation and aggregation would be further determined by the studies on salt bath and electrochemical behaviors, as discussed in the following sections.

The free standing film, or membrane of PMMA and PMMA/MMT nanocomposites used for the molecule barrier measurements has a thickness of about 30 μm. The gas permeability of oxygen and H_2O vapor is shown in Figure 5. Compared with PMMA membrane, free standing film of PMMA/MMT nanocomposites at relatively low clay loading (1.0 wt %) shows about 78% reduction of oxygen permeability. Meanwhile, compared to PMMA, this film at low clay loading (0.75%) also shows about 56.8% reduction of the H_2O vapor permeability. As shown in Figure 5, these results implied that while adding a small amount of modified MMT (0.5%) in the PMMA, there was a remarkable and immediate reduction of the oxygen and H_2O vapor permeability. However, it was also observed that the decline of oxygen and H_2O vapor permeability reached the lowest point at 1.0 and 0.75 wt % MMT loading, respectively. Then the oxygen and H_2O vapor permeability increased gradually as modified MMT loading increased, such as at 3.0 or 5.0 wt %. The cause might be because of the partial phase separation between the organic polymer and inorganic intercalated nanolayer of MMT.

Anticorrosive property of brass coated by PMMA/MMT nanocomposites

The simplest way to evaluate the anticorrosive property is the salt bath experiment, which was employed to observe the long term corrosion progress on the surface and to record when corrosion occurred. Table I shows the time corrosion occurred and that it affected 5% of the surface area of brass coupons, incorporated with and without the nanocomposites coating. Table I also shows that the corrosion progress of brass was postponed owing to the nanocomposites coating, especially in 1.0 wt %-coated coupon. With nanocomposites coating, the time was extended from 17 h (bare) to 527 h (1.0 wt %), indicating that its anticorrosive property was superior. Meanwhile, with regard to the corrosion progress of each coupon, the anticorrosive property of the 0.5, 0.75, and 1.0 wt %-coated coupons was better than those of the others.

The anticorrosive property of brass coated by nanocomposites was evaluated mainly from the values of corrosion current (i_{corr}), corrosion rate (R_{corr}) and polarization resistance (R_p).

From the cathodic and anodic scans, the peaks of i_{corr} observed at approximately −250 mV (versus SCE) could be attributed to the presence of copper chloride complex ($CuCl_2^-$) from brass alloy, because the presence of $CuCl_2^-$ is more stable than $ZnCl_2$. At a potential more noble than −250 mV (versus SCE), both Zn and Cu dissolve simultaneously out of the brass alloy surface at different rates.[17] The R_{corr}, i_{corr}, and corrosion potential (E_{corr}) are listed in Table II. Figure 6 shows the Tafel plot of each brass coupon. The brass coupons coated with PMMA/MMT nanocomposites showed lower value in R_{corr} and i_{corr} than did the coupons without nanocomposites, especially in 1.0 wt %-coated coupon. The i_{corr} of 1.0 wt %-coated coupons was about 6.86 nA/cm^2, whereas the i_{corr} of bare and PMMA-coated coupons were about 7340 and 223.3 nA/cm^2, respectively. Meanwhile, the R_{corr} of 1.0 wt %-coated coupons was about 0.103 $\times$ 10^{-3} mm/year, whereas the R_{corr} of bare and PMMA-coated coupons were about 110 and 3.36 $\times$ 10^{-3} mm/year, respectively. The results of i_{corr} and R_{corr} presented marked enhancement of the anticorrosive property of coupons coated with nanocomposites. Meanwhile, these results also implied that after adding

TABLE I
Under Salt Bath Experiment, the Time at Which Corrosion Occurred as a Function of MMT Loading in PMMA/MMT Nanocomposites

Compound code	The time passed until corrosion occurred (average, h)
No coating	17
PMMA	113
PMMA-0.5	395
PMMA-0.75	420
PMMA-1	527
PMMA-3	290
PMMA-5	281

TABLE II
Relations of the Composition of PMMA/MMT Nanocomposites with the E_{corr}, i_{corr}, R_p, and R_{corr}, Which is Measured from Electrochemical Methods (SCE was employed as reference electrode)

	Feed compostion (wt %)		Electrochemical measurements			
Compound code	Polymer	Modified MMT	E_{corr} (mV)	i_{corr} (nA/cm^2)	R_p ($\times 10^4$ Ω cm^2)	R_{corr} ($\times 10^{-3}$ mm/year)
Bare	0	0	−250.1	7340	0.93	110
PMMA	100	0	−244	223.3	10.15	3.36
PMMA-0.5	99.5	0.5	−252	193.4	13.23	2.91
PMMA-0.75	99.25	0.75	−350	98.6	27.23	1.48
PMMA-1	99	1	−272.1	6.86	58.14	0.103
PMMA-3	97	3	−246.4	27.06	14.18	0.407
PMMA-5	95	5	−252.7	29.87	15.16	0.45

a small amount of modified MMT in the PMMA matrix, there was a remarkable and immediate fall in the i_{corr} and R_{corr}. However, it was also observed that the decline of i_{corr} and R_{corr} reached the lowest point at 1.0 wt % MMT loading, and then increased gradually as modified MMT loading increased, such as at 3.0 or 5.0 wt %. The cause of the i_{corr} and R_{corr} increase might be due to the intercalation and aggregation phenomenon observed by XRD and TEM as above.

Consequently, to further evaluate the anticorrosive property of brass coated with nanocomposites, EIS was also employed to examine the activity difference between the brass surface after treatment with PMMA and PMMA/MMT nanocomposites. Figure 7(a,b) show the Nyquist plots of the brass coupons. The charge-transfer resistances of coupons can be determined by the intersection of the low-frequency end of the semicircle arc with the real axis. The enclosed area under each arc provides direct evidence for evaluating the anticorrosive property of each brass coupon. The one with the largest area shows the best anticorrosive performance. Figure 7(a) shows that 1.0 wt %-coated coupons had a larger enclosed area than did bare, PMMA, 0.5 and 0.75 wt %-coated coupons. Figure 7(b) also shows that 1.0 wt %-coated coupons had a larger enclosed area than did 3.0 and 5.0 wt %-coated coupons. It can be seen in Table I that the R_p of 1.0 wt %-coated coupons was also the largest, about 5.81×10^5 Ω°cm^2, whereas the R_p of bare, PMMA, 5.0 wt % coated coupons was about 0.093×10^5 Ω°cm^2, 1.01×10^5 Ω°cm^2, and 1.5×10^5 Ω°cm^2, respectively. As modified MMT loading increased, the anticorrosive property shot up sharply at the beginning but then reached a peak at 1.0 wt %, followed by markedly declining. The results of EIS concluded with the same tendency as the results of potentiodynamic polarization.

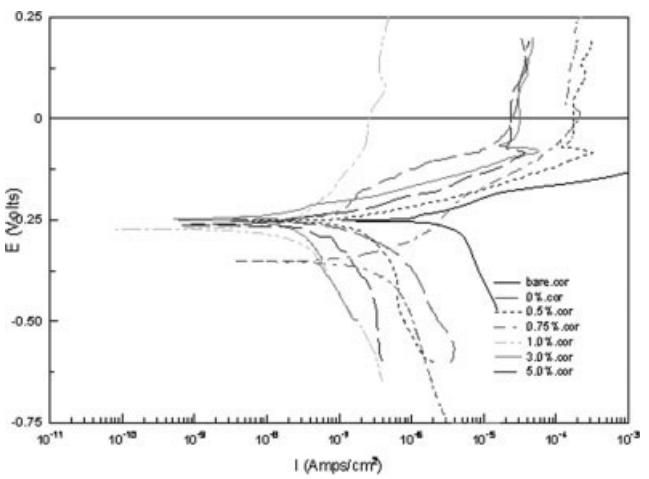

Figure 6 Tafel plots of bare, PMMA, 0.5, 0.75, 1.0, 3.0, and 5.0 wt %-coated brass coupon.

According to the results above, the gas permeability and the anticorrosive property, such as i_{corr} and R_p, of the brass coupons coated with PMMA were better than that of the bare ones. The anticorrosion mechanism of polymer film is such that forming a polymer coating as a physical barrier can prevent brass from corroding and being attacked by O_2, H_2O molecules, and other corrosive environments.[11] After adding modified MMT into the PMMA matrix, the anticorrosive property of the brass coupons coated with nanocomposites was further promoted, as listed in Table I. The enhancement of anticorrosion was contributed to by the fact that inorganic clay, such as MMT, with a plate-like shape and high-aspect ratio is able to effectively extend the diffusion pathways of O_2, H_2O, and Cl^- across the PMMA/MMT nanocomposites coating, as well as to decrease the permeability of the coating.[9,7,11] The model of diffusion pathways extension can be explained by the following eq. (3)[18]

$$d' = d + d\frac{LV_f}{2W} \tag{3}$$

where d is the ideal thickness of PMMA, L is the mean length of silicate layers, W is the mean thickness of silicate layers and V_f is the silicate layers' volume fraction of nanocomposites. The mean diffusion pathways of gas and liquid molecules are almost equal to d, the thickness of PMMA. In the

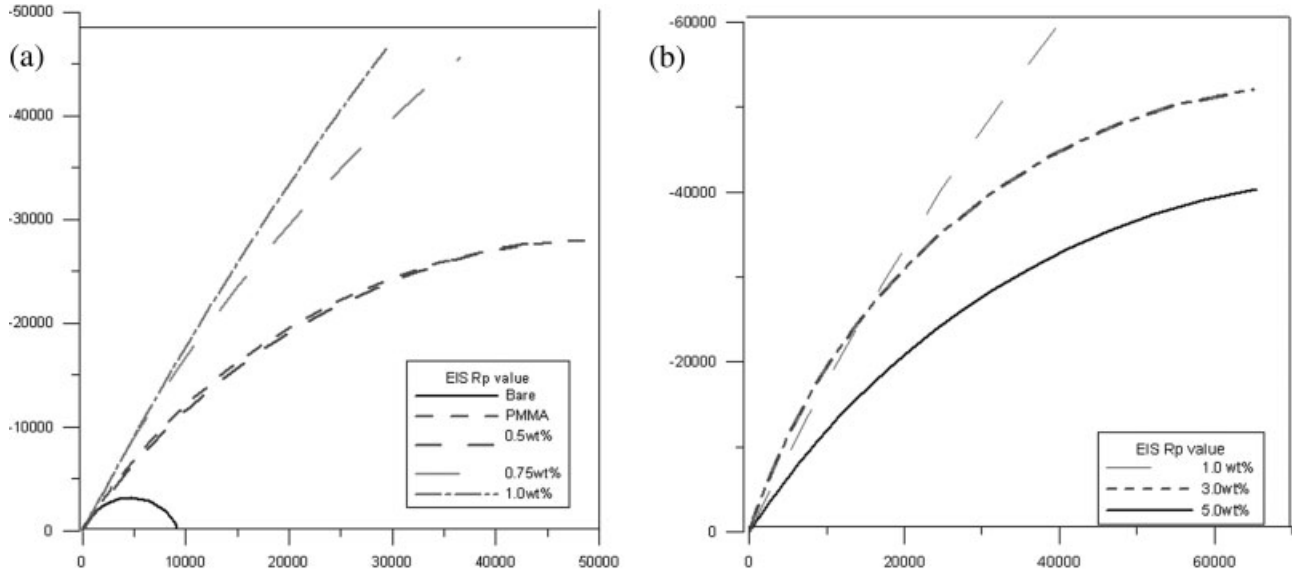

Figure 7 (a) Nyquist plots for bare, PMMA, 0.5, 0.75, and 1.0 wt %-coated brass coupon, measured in 5 wt % aqueous NaCl solution. (b) Nyquist plots for 1.0, 3.0, and 5.0 wt %-coated brass coupons measured in 5 wt % aqueous NaCl solution.

nanocomposites, the mean diffusion pathways of gas and liquid molecules, d', can be simply calculated by eq. (3). According to this equation, as the gas and liquid molecules diffuse across the nanocomposite materials, they have to detour around each well-dispersed silicate layer on a nanometer scale, which can efficiently extend their diffusion pathways. Moreover, the longer d' can be achieved with the higher V_f, indicating that these silicate layers can effectively minimize the R_{corr} of our brass coupons. Meanwhile, the anticorrosive property of nanocomposites should be further promoted with an increase of the modified MMT loading.

On the basis of the salt bath, potentiodynamic polarization and EIS experiments, it can be shown that after adding a small amount of modified MMT into the PMMA matrix, the anticorrosive property of brass was markedly promoted and reached the highest point at the amount of 1.0 wt % modified MMT, at which point the i_{corr} and R_p were 6.9 nA/cm^2 and 5.81 $\times$ 10^5 Ω°cm^2, respectively. As listed in Table III, the i_{corr} of brass coated with nanocomposites was two or even three orders smaller than when treated by other organic inhibitors, highlighting that the enhancement of the anticorrosive property of brass made by the PMMA/MMT nanocomposites coating, was much superior to that achieved with any organic inhibitor. Meanwhile, its R_p was also the strongest supporting evidence of its outstanding anticorrosive property.[19–22]

However, as modified MMT loading further increased, such as to 3.0 or 5.0 wt %, the gas permeability of nanocomposites increased and the anticorrosive property of the coating then steadily decreased. One cause of this decrease is that the silicate layers of modified MMT would intercalate or aggregate together because of the swelling of the PMMA molecules during the polymerization progress, which was observed by XRD and TEM. This phenomenon has been found and discussed in several papers.[14–16,23] This intercalation and aggregation would dismantle the exfoliated structure of the nanocomposites and then induce stress concentration, ending in a decrease of the anticorrosive property of brass coated with PMMA/MMT nanocomposites.

In this study, the anticorrosive property of 7Cu3Zn brass was promoted using PMMA/MMT nanocomposite coatings and increased as the modified MMT loading increased, until reaching a peak at 1.0 wt %-coated coupon. This means that the superior anticorrosive property of brass coated with nanocomposites can be achieved with only 1.0 wt %

TABLE III
Under the Optimum Conditions, the i_{corr} and R_p of Brass Coated with Nanocomposites Was Compared with Those Treated with Other Organic Inhibitors

Materials	i_{corr} (nA/cm^2)	R_p ($\times$ 10^4 Ω cm^2)
PMMA/MMT	6.9	58.14
DBMM	1100	15.84
HPBT	840	22.15
HBTA	650	40.1
BTA	1120	18.5
BTMA	2000	19.5
2-[(*E*)-pyridin-2-ylimino)methyl]phenol	290	16
2-[(pyridin-2-ylamino)methyl]phenol	470	12.6

of modified MMT, which is an extremely small amount, whereas the traditional composites usually need 30 wt % of filler to reinforce their matrix. Therefore, applying PMMA/MMT nanocomposite to minimize the corrosion of brass is very economical and efficient, and shows great potential for industrial applications in the future.

CONCLUSIONS

To improve the anticorrosive property of 7Cu3Zn brass, a series of PMMA/MMT nanocomposite coatings were prepared through the effective dispersion of the silicate layers of organophilic MMT in PMMA matrix via solution polymerization. On the basis of XRD, TEM observation, and after modified MMT was added, the *d*-spacing of its silicate layers increased, and the silicate layers of modified MMT were exfoliated during PMMA solution polymerization on a nanometer scale. Moreover, both exfoliation and intercalation were observed and found to be well-dispersed in nanocomposites. The anticorrosive property of brass coated with nanocomposites was superior and more protective than results attained by other techniques. After adding a small amount of modified MMT into the PMMA matrix, the i_{corr} and R_{corr} of brass declined sharply, while the gas permeability and R_p rose steadily, indicating that PMMA/MMT nanocompoistes indeed enhance the anticorrosive property of brass. However, as modified MMT loading further increased, the tendency of the anticorrosive property became opposite to its earlier reaction, since the silicate nanolayers of the modified MMT intercalate or even aggregate together easily during the polymerization process, and these locations of nanocomposites resulted in an increase in the corrosion susceptibility on the brass surface.

References

1. Elmorsi, M. A.; Hassanein, A. M. Corros Sci 1999, 41, 2337.
2. Assouli, B.; Ait Chikh, Z. A.; Idrissi, H.; Srhiri, A. Polymer 2001, 42, 2449.
3. Usuki, A.; Kawasumi, M.; Kojima, Y.; Okada, A.; Karauchi, T.; Kamigaito, O. J Mater Res 1993, 8, 1174.
4. Usuki, A.; Kawasumi, M.; Kojima, Y.; Okada, A.; Fakushima, Y.; Karauchi, T.; Kamigaito, O. J Mater Res 1993, 8, 1180.
5. Kojima, Y.; Usuki, A.; Kawasumi, M.; Okada, A.; Fakushima, Y.; Karauchi, T.; Kamigaito, O. J Mater Res 1993, 8, 1185.
6. Yeh, J.-M.; Liou, S.-J.; Lai, M.-C.; Chang, Y.-W.; Huang, C.-Y.; Chen, C.-P.; Jaw, J.-H.; Tsai, T.-Y.; Yu, Y.-H. J Appl Polym Sci 1936, 2004, 94.
7. Yeh, J.-M.; Liou, S.-J.; Lai, M.-C.; Wu, P.-H. Chem Mater 2001, 13, 1131.
8. Yu, Y.-H.; Yeh, J.-M.; Liou, S.-J.; Chen, C.-L.; Liaw, D.-J.; Lu, H.-Y. J Appl Polym Sci 2004, 92, 3573.
9. Yu, Y.-H.; Jen, C.-C. J Appl Polym Sci 2004, 91, 3438.
10. Morgan, A. B.; Gilman, J. W.; Jackson, C. L. Macromolecules 2001, 34, 2735.
11. Kim, J.-K.; Hu, C.-G.; Woo, R. S. C.; Sham, M.-L. Compos Sci Technol 2005, 65, 805.
12. Yeh, J.-M.; Liou, S.-J.; C. Lin, C.; Chen, C.-P.; Chang, Y.-W. Chem Mater 2002, 14, 154.
13. Chi, T.-N.; Shang, W.-Y. In PLS Nano Composite Materials, 1st ed.; Yang, R.-T., Ed.; Wu-nan: Taipei, 2004; Chapter 3, p 76.
14. Qu, X.-G.; Guan, R.-T.; Liu, G.-D.; She, Q.-G.; Zhang, L.-C. J Appl Polym Sci 2005, 97, 348.
15. Wan, C.-Y.; Qiao, X.-Y.; Zhang, Y. J Appl Polym Sci 2003, 89, 2184.
16. Khalil, H.; Mahajan, D.; Rafailovich, H. Polymer Int 2005, 4, 428.
17. Al-kharafi, F. M.; Ateya, B. G.; Abd Allah R. M. J Appl Polym Sci 2004, 34, 47.
18. Neilsen, L. E. J Macromol Sci A1 (Chem) 1967, 5, 929.
19. Ravichandran, R.; Rajedran, N. Appl Surf Sci 2005, 241, 449.
20. Nagiub, A.; Manfield, F. Corros Sci 2001, 43, 2147.
21. Ravichandran, R.; Nanjundan, S.; Rajedran N. Appl Surf Sci 2004, 236, 241.
22. Asan, A.; Kabasakalogu, M.; Isiklan, M.; Kilic, Z. Corros Sci 2005, 47, 1534.
23. Mani, G.; Fan, Q.-G.; Samuel C. U.; Yang, Y. J Appl Polym Sci 2005, 97, 218.